Published in final edited form as:
*Clin Cancer Res*. 2010 February 1; 16(3): 1049. doi:10.1158/1078-0432.CCR-09-1997.

# Clinical Pharmacokinetics of Amifostine and WR1065 in Pediatric Patients with Medulloblastoma

**Trevor McKibbin**[1], **John C. Panetta**[2,3], **Maryam Fouladi**[4], **Amar Gajjar**[4], **Feng Bai**[2], **M. Fatih Okcu**[5], and **Clinton F. Stewart**[1,2]

[1]Department of Clinical Pharmacy, University of Tennessee, Memphis, TN

[2]Department of Pharmaceutical Sciences, St. Jude Children's Research Hospital (SJCRH), Memphis, TN

[3]Department of Pharmaceutical Sciences, University of Tennessee, Memphis, TN

[4]Department of Oncology, St. Jude Children's Research Hospital, Memphis, TN

[5]Texas Children's Cancer Center; Department of Pediatrics, Hematology-Oncology, Baylor College of Medicine, Houston, TX

## Abstract

**Purpose—**We evaluated the pharmacokinetics of amifostine and WR1065 in pediatric patients with newly diagnosed medulloblastoma, to assess the influence of patient covariates, including demographics, clinical characteristics, and genetic polymorphisms, on amifostine and WR1065 pharmacokinetic parameters.

**Experimental design—**We assessed the pharmacokinetics of amifostine and WR1065 in 33 children who received amifostine (1 min infusion, 600 mg/m$^2$) just prior to the start of and 3 hours into a 6-hour cisplatin infusion. Serial blood samples were collected after doses 1 (0 hr) and 2 (3 hr) of course 1. Amifostine and WR1065 were quantitated by HPLC with electrochemical detection. A pharmacokinetic model was simultaneously fit to amifostine and WR1065 plasma or whole blood concentration-versus-time data. The influence of demographic, biochemical, and pharmacogenetic covariates on amifostine and WR1065 disposition was evaluated.

**Results—**Body surface area was the primary size-based covariate for amifostine pharmacokinetics explaining 53% and 56% of interindividual variability in plasma and whole blood amifostine clearance, respectively. The population predicted values for amifostine clearance, volume, and apparent WR1065 clearance from the plasma data were: 107 L/hr/m$^2$, 5.53 L/m$^2$, and 30.6 L/hr/m$^2$. The population predicted values for amifostine clearance, volume, and apparent WR1065 clearance from whole blood data were 136 L/hr/m$^2$, 7.23 L/m$^2$, and 12.5 L/hr/m$^2$.

**Conclusions—**These results support using body surface area for calculating doses of amifostine in children. Similar to data in adults, amifostine and WR1065 are rapidly cleared from plasma and whole blood in children.

### Keywords

Pharmacokinetics; pediatrics; amifostine; pharmacogenetics; WR1065

Address for Correspondence and reprints: Clinton F. Stewart, Pharm. D., Pharmaceutical Department, St Jude Children's Research Hospital, 262 Danny Thomas Place, Memphis TN 38105-2794 Telephone: (901) 595-3665; FAX: (901) 525-6869 clinton.stewart@stjude.org.

## Introduction

Medulloblastoma is the most common childhood central nervous system malignancy (1). The use of cisplatin for the treatment of medulloblastoma has improved overall survival and enabled the use lower doses of cranial spinal irradiation (2,3). However, cisplatin carries with it a host of both short-term and long-term toxicities including significant ototoxicity. Approximately 35% of children treated with cisplatin for medulloblastoma have significant ototoxicity (2,4). Amifostine significantly reduces the risk of severe ototoxicity in patients with average-risk medulloblastoma receiving dose-intense chemotherapy when administered before and during the cisplatin infusion (5).

Amifostine is a prodrug converted to the active thiol metabolite WR1065, which acts as a nonspecific cytoprotectant, reducing the toxicity associated with alkylating agents and radiation therapy by scavenging free radicals (6). The conversion of amifostine to WR1065 is catalyzed by alkaline phosphatase and is pH dependent, occurring more rapidly in alkaline pH. The lower concentration of membrane-bound alkaline phosphatase and lower pH in tumor environments contribute to a relatively low concentration of active chemoprotectant in malignant tissues, providing a relatively selective cytoprotection of normal tissues (7–9). The half-life of amifostine is approximately 9 minutes, whereas that of the active metabolite, WR1065, is approximately 15 minutes. Thus, the schedule of amifostine administration is potentially an important factor for optimum efficacy (7,10,11).

Despite a promising mechanism of action for selective protection of normal tissues, investigations of the cytoprotective effects of amifostine have yielded mixed results (5,12, 13). These conflicting findings may be related to differences in the schedule and dosage of amifostine, inadequate statistical power, and differences in the underlying chemotherapy and patient populations studied. Fouladi and colleagues conducted a phase 1 evaluation of amifostine in combination with a 6 hour cisplatin infusion and concluded the optimum schedule was 600 mg/m$^2$ just prior to and 3 hours into a 6 hour cisplatin infusion (14). This schedule of administration significantly reduced the ototoxicity associated with the treatment of medulloblastoma (5). To date, investigations of the pharmacokinetic parameters of amifostine and WR1065 in pediatric patients remain limited.

Amifostine and WR1065 are involved in a complex interaction with the glutathione pathway. In vitro exposure of cells to WR1065 results in increased precursor uptake and biosynthesis of glutathione (15). Additionally, the elimination of WR1065 may be partially mediated as a glutathione conjugate (16). Significant functional polymorphisms in the glutathione *S*-transferase (GST) pathway have been discovered, with implications for the clearance of multiple drugs including chemotherapeutics (17–20). These polymorphisms include *GSTM1*0*, in which the gene is deleted. Homozygous patients express no M1 protein. *GSTT1* is also polymorphic with homozygotes lacking GST T1 function. The GSTP1 polymorphism involves a single nucleotide polymorphism resulting in an amino acid substitution. A resulting steric effect on substrate binding causes substrate specific functional effects (17,21). Evaluating functional polymorphisms as covariates for pharmacokinetic parameters may help to explain variability in amifostine and WR1065 clearance.

Analytical procedures for measuring amifostine and WR1065 have been developed for both plasma and whole-blood. To date, it is not known which sampling matrix provides a better model for relating pharmacokinetics to pharmacodynamics (10,11,16). WR1065 is rapidly auto-oxidized creating a scenario in which sample preparation and procedures for arresting oxidation may have significant implications for the concentrations measured (10,16,22). The analytical procedure used in this investigation permitted simultaneous bioanalytical measurements in both blood and plasma (23).

The objectives of this investigation were to: 1) simultaneously assess the pharmacokinetics of amifostine and WR1065 in pediatric patients treated with cisplatin for medulloblastoma, 2) estimate the magnitude of interpatient pharmacokinetic variability along with individual estimates of patient pharmacokinetic parameters, 3) investigate the effects of baseline clinical variables and functional polymorphisms of GST M1, T1, and P1 on the variability of the pharmacokinetic parameters, 4) evaluate parameter estimates derived from whole blood and plasma sampling in relation to pharmacodynamic effects of amifostine, and 5) use the current dataset to develop a limited sampling model (LSM) for future investigations of amifostine pharmacokinetics.

## METHODS

### Patients and treatment

The population pharmacokinetic analysis included amifostine and WR1065 plasma and whole blood concentration-time data from children that participated in the protocol St Jude Medulloblastoma [SJMB]-96 (5,24). Eligibility criteria included: patients aged ≥ 3 and ≤ 21 years old at the time of diagnosis who had not previously received chemotherapy or irradiation. Prior corticosteroid therapy was allowed. Patients were required to begin treatment within 28 days of definitive surgery. Medulloblastoma risk category was classified according to a modified Chang staging system, as previously described (24). Additional eligibility criteria included normal renal function, normal liver function, normal bone marrow function (hemoglobin ≥ 10 g/dL, WBC count ≥ 3,000/mL, absolute neutrophil count [ANC] ≥ 1,500/mL, and platelets ≥ 100,000/$mm^3$), and an the Eastern Cooperative Oncology Group (ECOG) performance score of 0 to 3, except in cases of posterior fossa syndrome. Informed consent was obtained from the parent/guardian or patient per the St. Jude Children's Research Hospital Institutional Review Board.

All patients underwent an attempt at maximal surgical resection of the tumor and received treatment with radiation and chemotherapy as previously described (24). After a 6-week rest period, patients began four cycles of high-dose chemotherapy, each followed by stem-cell or bone marrow rescue. The high-dose chemotherapy included cisplatin 75 mg/$m^2$, vincristine 1.5 mg/$m^2$ (2 mg max) on day −4, followed by cyclophosphamide 2 gm/$m^2$ continuous infusion with MESNA on days −3 and −2, hydration on day −1 and infusion of peripheral blood stem cells or bone marrow on day 0, with supportive care and filgrastim in the following days and a subsequent dose of vincristine 1.5 mg/$m^2$ (2 mg max) on day +6. Amifostine 600 mg/$m^2$ was administered with each cycle of cisplatin containing chemotherapy as a 1-minute intravenous infusion just prior to the start and 3 hours into the 6-hour cisplatin infusion.

### Blood and plasma sampling and bioanalysis

Samples were obtained pre infusion, 2, 5, 10, 30, 60, 120, and 180 minutes after both the first and second amifostine dose during course one of cisplatin. Plasma and whole blood concentrations of amifostine and WR1065 were assayed as previously described (23). In short, for each sample the concentration of native WR1065 was determined. To measure the concentration of amifostine, a sample was incubated for 4 hours at 37° C to convert amifostine to WR1065. After incubation, the sample was assayed to determine the concentration of WR1065. This concentration of WR1065 represented the concentration of amifostine (converted) plus the native WR1065 previously assayed. Subtraction of the native WR1065 concentration from the converted WR1065 determined the concentration of amifostine. The lower limit of quantitation (LLQ) of amifostine and WR1065 was 0.25 μM. The bioanalytical procedure was performed for both whole blood and plasma for each sampling time.

### Pharmacogenetic analysis

We hypothesized the no or low activity GST genotypes (*GSTP1*A, GSTM1 null*, and *GSTT1 null*) would result in altered systemic clearance of amifostine and WR1065. We used a multiplex polymerase chain reaction (PCR) technique to amplify both *GSTM1* and *GSTT1* simultaneously in a single PCR reaction as described in detail before (25). In analyses, patients with null genotypes were compared with patients with nonnull genotypes. We determined *GSTP1* rs1695 and rs1138272 polymorphisms by PCR and RFLP methods as described before (25). We analyzed the *GSTP1* results by comparing patients with the **A*/**A* genotype with the rest of the group, who had at least one variant allele. For quality control, 10% of all of the samples were repeated.

### Pharmacokinetic analysis

The pharmacokinetics of amifostine and WR1065 were determined by nonlinear mixed-effects modeling via NONMEM (version VI, GloboMax LLC, Hanover, MD), using the first-order conditional estimation method (FOCE) with INTERACTION via the ADVAN7 subroutine (26). Plasma and whole blood concentration time data were modeled separately. Xpose (27), Census (28), and R-project (version 2.8.1) were used for data management and visualization. Posterior Bayesian individual estimates of amifostine and WR1065 pharmacokinetic parameters were obtained within NONMEM. The pharmacokinetic parameters estimated included amifostine systemic clearance ($CL_{am}$), volume of distribution (VD), amifostine intercompartmental rate constants $k_{12}$, and $k_{21}$, apparent clearance of WR1065 ($CL_{WR}$), and WR1065 intercompartmental rate constants $k_{wr34}$ and $k_{wr43}$ (Figure 1). The pharmacokinetic model assumed the VD of amifostine was equal to the VD of WR1065.

The distribution of parameters was assumed to be log-normal. Both interindividual (IIV) and interoccasion (IOV) variability in parameters were modeled as exponential terms. An occasion was defined as one dosing occasion of amifostine. The residual errors for amifostine and WR1065 were each modeled independently using a mixed proportional and additive error model:

$$Cp_{ik}=\widehat{C}p_{ik}\left(1+\varepsilon_{ik}^{rel}\right)+\varepsilon_{ik}^{abs}$$

where $Cp_{ik}$ and $\widehat{C}p_{ik}$ represent the $k^{th}$ actual and predicted concentrations in individual $i$, respectively. The error terms $\varepsilon^{rel}$ and $\varepsilon^{abs}$ are the components of the proportional and additive error, respectively. The proportional error was assumed to have a mean of zero and variance of $\sigma$. The components of additive error for amifostine and WR1065 were both fixed to 0.25 in consideration of the LLQ of the assay (0.25 μM). Observed amifostine and WR1065 concentrations below the LLQ were substituted with 0.125 (1/2*LLQ).

Covariates considered in the analysis included body surface area (BSA), age, gender, race, albumin, total bilirubin, GST polymorphisms (M1, T1, and P1), serum creatinine, and calculated glomerular filtration rate (29). A covariate was considered significant in this analysis if the addition of the covariate to the model reduced the objective function value (OFV) at least 3.84 units ($P < 0.05$, based on the $\chi^2$ test for the difference in the −2 log-likelihood between two hierarchical models that differ by 1 degrees of freedom).

The relationships between the pharmacokinetic parameters ($CL_{am}$, VD, and $CL_{WR}$) and categorical or continuous covariates were described using the following model:

$$\theta = \tilde{\theta} + \sum_{\rho=1}^{m} \text{covariate}_{\rho} \times \theta_{\rho}$$

where θ was the population estimate, $\tilde{\theta}$ was the population estimate with none of the covariates included, and θρ was the effect of covariate ρ on the model. When a categorical variable was considered, the presence of a covariate was coded as covariate ρ = 1 and its absence as covariate ρ = 0. When sex was evaluated as a covariate male patients were coded as ρ = 0 and females as ρ = 1. Patients with incomplete data were censored when covariate analysis included variables for which data were missing.

Bootstrap analysis was used to evaluate robustness of models and calculate standard error estimates and 95% confidence intervals for parameters (30). The nonparametric bootstrap procedure utilized random sampling from the data used for building the base population pharmacokinetic model with replacement to create bootstrap data sets (*n*=500) with the same sample size as the original. Each new data set was fit to the final model and population variables were estimated. This procedure was performed separately for the plasma and whole blood data sets.

## Pharmacodynamic Assessment

The primary adverse events of amifostine are hypotension, nausea, and hypocalcemia related to transient hypoparathyroidism (5). We sought to determine whether parameter estimates derived from whole blood and plasma sampling blood would provide a more robust model in relating pharmacokinetic assessments to pharmacodynamic effects of amifostine (hypocalcemia and hypoparathyroidism). The decrease from baseline and duration of decrease in ionized calcium values and parathyroid hormone values was used to assess relationships between pharmacokinetic parameters and toxicity with both plasma and whole blood derived data. Sampling of ionized calcium and parathyroid hormone was performed prior to and during the 24 hours after the amifostine infusion.

## Selection of pharmacokinetic limited sampling model (LSM)

We used the plasma amifostine and WR1065 data to create a limited sampling model for use in future clinical trials of amifostine. The LSM was determined using the estimated population pharmacokinetic parameters in the plasma data. A stepwise process was used to determine an adequate limited sampling model that would estimate individual post-hoc amifostine systemic clearance, volume of distribution, and apparent WR1065 clearance. The following sampling strategies were evaluated: 2 samples from one amifostine dose or occasion (5 and 30 minutes), 2 samples from each of 2 occasions (5 and 30 minutes), 3 samples from 1 occasion (5, 30, and 60 minutes), and 3 samples from each of 2 occasions (5, 30, and 60 minutes).

The following process was used to evaluate limited sampling strategies. First, the concentration time data were limited to the sampling times of interest. The individual post hoc estimates were obtained in NONMEM with each of the limited sampling datasets using the population estimates from the final BSA-normalized plasma model as population priors. This process was repeated for each sampling strategy evaluated. The individual post hoc estimates from each limited sampling strategy were then compared to the post hoc estimates from the full base model and the relative bias and accuracy calculated.

The Wilcoxon Signed-Rank test was used to compare individual post hoc estimates from each of the limited sampling strategies to the post hoc estimates from the full base model. All statistical tests used a two-tailed significance threshold of $p<0.05$ without correction for

multiple testing. Statistical analyses were carried out using JMP® software v7.0.1 (SAS Corp., Gary, NC).

# RESULTS

## Patient population

Of the 134 patients that underwent treatment on the protocol SJMB-96 and received amifostine, 49 consented to participate in the pharmacokinetic studies. One patient enrolled in pharmacokinetic studies was unable to contribute samples due to hypotension related to amifostine administration. During WR1065 assay development, it was determined that because of WR1065 instability, samples assayed greater than 48 hours after collection were not evaluable (23). This restriction created a dataset with 33 patients with 649 evaluable whole blood samples and 33 patients with 711 evaluable samples in plasma. Baseline patient characteristics of the patients with pharmacokinetic sampling were comparable to those of the full clinical trial population(24) and are provided in Table 1.

## Amifostine and WR1065 disposition

Results from pharmacokinetic studies of amifostine and WR1065 in adult patients showed that a four compartment model adequately described their disposition (10). We also used a model with a total of four compartments to simultaneously model amifostine (two compartments) and WR1065 (two compartments) with a rate constant describing the conversion of amifostine to WR1065 (Figure 1).

Using the plasma amifostine and WR1065 concentration-time data, the amifostine population pharmacokinetic parameter estimates included $CL_{am}$, VD, $k_{12}$, and $k_{21}$, and were 107 L/h, 5.62 L, 3.02 $h^{-1}$, and 4.99 $h^{-1}$, respectively (Table 2). Population pharmacokinetic parameters of plasma WR1065 included $CL_{WR}$, $k_{34}$, and $k_{43}$, and were 30.1 L/h, 55.3 $h^{-1}$, and 14.3 $h^{-1}$, respectively.

The same structural model was used for the whole blood amifostine and WR1065 concentration-time data. The whole blood amifostine pharmacokinetic parameter estimates included $CL_{am}$, VD, $k_{12}$, and $k_{21}$ and were 135 L/h, 7.14 L, 4.16 $h^{-1}$, and 4.13 $h^{-1}$ (Table 2). Population pharmacokinetic parameters of WR1065 from whole blood data were 12.7 L/h, 25.1 $h^{-1}$, and 12.9 $h^{-1}$ for $CL_{WR}$, $k_{34}$, and $k_{43}$, respectively.

The plasma and whole blood estimates of IIV for amifostine clearance were 56% and 55%, respectively. The respective plasma and whole blood estimates of IIV for WR1065 apparent clearance in plasma and whole blood were 58% and 39%. The proportional components of residual variability for amifostine and WR1065 in the plasma model were 0.14 (37%) and 0.19 (44%), respectively. The values for proportional residual variability in the whole blood model for amifostine and WR1065 were nearly identical; 0.13 (36%) and 0.19 (44%), respectively.

We considered BSA and weight as possible size-based covariates. BSA was found as a significant determinant of $CL_{am}$ and VD, explaining 52% and 63% of the IIV, respectively (decrease in objective function value, DOFV = −24, $P < 0.001$) in the plasma model (Figure 2). A similar result was obtained in the whole blood model with BSA explaining 57% and 65% of the IIV for clearance and volume of amifostine, respectively (DOFV = −28, $P < 0.001$). Weight was also found to be a significant determinant of $CL_{am}$ and VD in plasma and whole blood models (DOFV = −22 and −27, $P < 0.001$). However, this change in the objective function was smaller than that observed when comparing the base model to the BSA-normalized data. Moreover, considering weight as a covariate explained 46% and 62% of the respective IIV in systemic clearance and volume of amifostine in plasma, which although significant was not as

much of an effect as BSA. Thus, BSA normalization was incorporated in the base model and remained in all subsequent analyses of the population model.

The estimates of IOV for amifostine systemic clearance were 19% and 27% in the respective plasma and whole blood BSA-normalized models. Inclusion of IOV decreased the objective function value by 32 and 71 in the respective plasma and whole blood models. The addition of IOV to the plasma model decreased the estimate of proportional residual error for amifostine from 0.19 (44%) to 0.13 (36%) (Table 3). In the BSA-adjusted whole blood model, the addition of IOV decreased the estimate of proportional residual error for amifostine from 0.33 (57%) to 0.19 (44%). The BSA-normalized model with IOV was used to screen each additional covariate in both plasma and whole blood data.

Of the three GST polymorphisms evaluated, the *GST P1* polymorphism provided the most promising results. Addition of the *GST P1* polymorphism to the plasma model (homozygous vs. variant) decreased IIV by 2.5%, but the change in objective function did not reach statistical significance (DOFV = −3.1, P= 0.08). None of the other GST polymorphisms resulted in significant decreases in measures of variability or improved diagnostic plots when evaluated in relation to amifostine or WR1065 pharmacokinetics in either the plasma or whole blood models.

In the covariate modeling, sex was found as a significant determinant of amifostine systemic clearance but not volume or WR1065 apparent clearance in the plasma model (DOFV = −7.4, P = 0.007). The estimated typical amifostine clearance in the plasma model was 99 L/hr/$m^2$ and 123 L/hr/$m^2$ in males and females, respectively (Table 2). The addition of sex to the model in whole blood data did not result in a decrease of the objective function value or IIV. In addition, including sex as a covariate in the whole blood based model did not change the estimate of residual proportional error for amifostine or WR1065 (Table 3).

The model predicted and individual predicted concentrations vs. observed concentrations of amifostine/WR105 in plasma and whole blood using the final model are represented as scatterplots in Supplementary Figures S1 and S2. Considering that the model predictions were symmetrically distributed around the line of identity, we conclude that the BSA-normalized model with IOV adequately describes amifostine and WR1065 disposition. The population pharmacokinetic concentration-time curves from the final models as well as observed values for amifostine and WR1065 concentrations are displayed in Figure 3. The intercompartmental rate parameter estimates ($k_{12}$, $k_{21}$, $k_{34}$, and $k_{43}$) from the initial and final models are available in Supplementary Table S3.

## Pharmacodynamic Assessment

We sought to develop a model to investigate the relationships between plasma and whole blood derived amifostine and WR1065 pharmacokinetic parameters and drug effect, namely hypocalcemia and parathyroid hormone values. A total of 32 patients had baseline and follow-up ionized calcium measurements. Of these patients, 12 (38%) had a decrease in serum ionized calcium to below 1 mM (normal range: 1.12–1.31 mM). Of these 32 patients, 31 received calcium chloride infusions either to prevent or as a result of hypocalcemia. Visual inspection of the change and duration of change in ionized calcium values did not reveal any relationships between this marker of drug effect and pharmacokinetics of amifostine and WR1065 in plasma or whole blood.

Baseline PTH values were available in 18 patients. All but one of the patients with measurements dropped below the level of detection for the assay (10 pg/mL), and only 7 patients had adequate sampling to determine a time to recovery; all of these patients recovered to normal values within 18 to 24 hours (Supplementary Figure S4). An additional 5 patients

had sampling out to 19 hours post amifostine, but had not yet recovered to the normal range. Visual inspection of the parathyroid hormone measurements did not reveal any relationships between this pharmacodynamic marker and plasma or blood pharmacokinetics.

### Limited Sampling Model

Data from 33 patients were used to create a pharmacokinetic limited sampling model to enhance the ability conduct studies of amifostine disposition in patient populations. The median biases for $CL_{am}$, and $CL_{WR}$ from the LSM with 2 samples (5 minutes and 30 minutes) from one amifostine dose (occasion) were 3.6% (Standard Deviation [SD], 46), and 30.7% (SD, 60), respectively. When a third sample was added (1 hour) to the one occasion sampling strategy, the bias estimates for $CL_{am}$ decreased to 3% (SD, 52) but increased to 37% (SD, 52) for apparent WR1065 clearance.

When a second occasion was added to the 2 sample strategy (total of 4 samples) the biases for $CL_{am}$ and $CL_{WR}$ were −1.24% (SD, 15), and −9% (SD, 46), respectively. For the strategy that required 3 samples on each of two occasions the mean biases for $CL_{am}$ and $CL_{WR}$ were 0.2% (SD, 12.2) and 13% (SD, 24), respectively. Of the models evaluated, the LSM with 2 samples from two occasions and 3 samples from two occasions resulted in the lowest calculated biases and were further compared to each other. The estimates of individual pharmacokinetic parameters were not significantly different between these two models for both $CL_{am}$ ($P = 0.8$) and $CL_{WR}$ ($P = 0.9$).

For all of the limited sampling strategies evaluated, the individual parameter estimates for amifostine systemic clearance were not statistically significantly different from those obtained with the full data set. However, the estimates for WR1065 apparent clearance from the LSM with 2 samples and 3 samples from one occasion were significantly different when compared to those obtained from the full model, p-values <0.0001 for both. Similarly, the estimates for WR1065 apparent clearance from the LSM with 2 samples from two occasions and 3 samples from two occasions were also significantly different from the parameters derived from the full dataset with respective p-values of 0.005 and 0.001.

## Discussion

This is the first population analysis of amifostine and WR1065 pharmacokinetics in a pediatric population. This analysis used a validated bioanalysis technique to measure amifostine and WR1065 in both plasma and whole blood and took advantage of the availability of sampling from both plasma and whole blood to model the data from both analytical matrices (23). The analysis identified a large component of variability between subjects and occasions, indicating large differences in exposure among different patients administered the same dosage. Body surface area was identified as the primary size-based covariate, explaining 52% and 57% of the variability in amifostine clearance in the plasma and whole blood models, respectively.

Gender was identified as a significant predictor of amifostine clearance in the plasma model. Possible explanations for the more rapid decline in plasma amifostine in female patients compared to male patients include: potential differences in metabolism, females may have a faster distribution of drug from serum to tissue that is not yet saturated, or there might be a slower redistribution back to blood from peripheral tissues in post infusion. This finding was not confirmed when modeled in the whole blood data. Lacking a specific mechanism that explains these results, the differences in clearance between male and female children observed in the plasma data requires further evaluation in future investigations.

WR1065 has several potential pathways for elimination; it may undergo auto-oxidation and may form bonds with mixed disulfides. Among the potential pathways of elimination is

conjugation with glutathione (16). We evaluated three functional polymorphisms in the glutathione pathway, none of which significantly explained variability in the pharmacokinetics of amifostine or WR1065. This may be because other pathways are available for the elimination of WR1065, or because with 25 patients with evaluable genotyping, this analysis was unable to elucidate all significant explanatory variables. Addition of *GSTP1* genotype as a covariate for systemic amifostine plasma clearance resulted in a trend, but was not statistically significant. Inclusion of *GSTP1* genotype in future investigations of amifostine and WR1065 pharmacokinetics may clarify the role of glutathione pathway polymorphisms in amifostine distribution.

We sought to evaluate the plasma derived and whole blood derived pharmacokinetic estimates in regard to their relationships with measures of the pharmacodynamic effects of amifostine, specifically, hypocalcemia and hypoparathyroidism. As this dosage of amifostine reliably resulted in hypocalcemia, many patients received calcium in a preventative manner, prior to amifostine. Administration of calcium can also influence parathyroid hormone levels, potentially masking pharmacokinetic and pharmacodynamic relationships. Nearly all patients with parathyroid hormone level measurements dropped below the level of quantitation for the clinical assay used. Thus, the measures of ionized calcium and parathyroid hormone measurements were insufficient to accurately model the pharmacodynamic effects of amifostine. These data highlight the difficulty of pharmacodynamic modeling in the complex milieu of the clinical environment and illustrate the need for early interim analyses to identify potential problems with study measures.

Overall, other than the WR1065 component, the plasma and whole blood models resulted in similar parameter estimates. Expression of alkaline phosphatase, the enzyme that catalyzes the conversion of amifostine to WR1065, on nucleated blood cells may have contributed to the slightly higher typical value of amifostine systemic clearance and the lower typical apparent clearance of WR1065 in the whole blood (31). A previous investigation of amifostine concentrations in the whole blood, plasma, and blood elements of five patients reported similar WR1065 concentrations in plasma, whole blood, and blood cells (32,33). While our data suggested higher concentrations of WR1065 in the whole blood compared to plasma. These disparate findings may be related to differences in analytical procedures, such as the methods used to arrest the oxidation of WR1065. Our methods included optimizing perchloric acid concentrations and the immediate immersion of samples into ice to decrease auto-oxidation (23).

The lack of a validation cohort may be considered a limitation to this investigation. However, the same structural model was used to separately fit data derived from plasma and whole blood sampling. Further investigations would be required to determine whether plasma or whole blood would provide more robust data in relation to drug effect. However, because the majority of estimates were similar in both matrices, either matrix is likely to be suitable for assessing drug distribution and effect.

As expected, the limited sampling strategy with the most sampling time points (total of 6 samples) resulted in the lowest measures of bias for amifostine clearance. The LSM with two samples (5 minutes and 30 minutes) drawn from two dosing occasions resulted in a similarly low bias estimate for amifostine clearance and a lower bias estimate for WR1065 apparent clearance. In addition, the parameter estimates from the LSM with two samples from two occasions were not significantly different from the LSM with 6 samples. With 33% fewer samples required, the LSM with two samples from two occasions would be preferable in future pharmacokinetic investigations of amifostine. While sampling from one occasion would likely provide accurate estimation of systemic amifostine clearance and volume, the estimation of

WR1065 apparent clearance using one occasion sampling models resulted in a large bias compared to the full sampling model.

In summary, we have developed a population pharmacokinetic model of amifostine and WR1065 in pediatric patients with medulloblastoma. We analyzed for the effects of covariates on amifostine pharmacokinetics using a nonlinear mixed effects approach. In the present analysis, we identified body surface area as a covariate that can be used prospectively in a model to predict amifostine clearance. This analysis identified a large component of interpatient variability in clearance of both amifostine and WR1065 which may have significant implications for this clinically important therapy.

**Summary of translational relevance describing how this work might be applied to the future practice of cancer medicine**

Currently, little is known regarding the pharmacokinetics of amifostine or its active metabolite WR1065 in children with cancer or about the factors that explain the interpatient variability of these pharmacokinetic parameters. This analysis has defined the disposition of amifostine and WR1065 in children with medulloblastoma. Further, this study investigated the relationship between expression of drug-metabolizing or transporter genotypes and disposition of amifostine and its primary metabolite. The covariate analysis has identified patient covariates, including body surface area, that are related to the pharmacokinetic parameters and explain the interpatient variability in these parameters.

## Supplementary Material

Refer to Web version on PubMed Central for supplementary material.

## Acknowledgments

The authors would like to thank Lisa Walters, Terri Kuehner, Sheri Ring, Margaret Edwards, and Paula Condy for their commitment to improving patient care and their assistance in obtaining patient samples. Additionally, we would like to thank Mark N. Kirstein and Susannah E. Motl-Moroney for their assistance in conducting this study.

This work was supported in part by the National Institutes of Health Cancer Center Support [CORE] Grant P30 CA21765, Pediatric Brain Tumor Foundation, Musicians Against Childhood Cancer (MACC), the Noyes Brain Tumor Foundation, Ryan McGhee Foundation, and the American Lebanese Syrian Associated Charities (ALSAC).

## References

1. Hughes EN, Shillito J, Sallan SE, Loeffler JS, Cassady JR, Tarbell NJ. Medulloblastoma at the joint center for radiation therapy between 1968 and 1984. The influence of radiation dose on the patterns of failure and survival. Cancer 1988;61:1992–8. journal. [PubMed: 3129177]
2. Gottardo NG, Gajjar A. Chemotherapy for malignant brain tumors of childhood. J Child Neurol 2008;23:1149–59. [PubMed: 18952581]
3. Kortmann RD, Kuhl J, Timmermann B, et al. Postoperative neoadjuvant chemotherapy before radiotherapy as compared to immediate radiotherapy followed by maintenance chemotherapy in the treatment of medulloblastoma in childhood: results of the German prospective randomized trial HIT '91. IntJ RadiatOncol BiolPhys 2000;46:269–79.
4. Bertolini P, Lassalle M, Mercier G, et al. Platinum compound-related ototoxicity in children: long-term follow-up reveals continuous worsening of hearing loss. J Pediatr Hematol Oncol 2004;26:649–55. [PubMed: 15454836]
5. Fouladi M, Chintagumpala M, Ashley D, et al. Amifostine protects against cisplatin-induced ototoxicity in children with average-risk medulloblastoma. J Clin Oncol 2008;26:3749–55. [PubMed: 18669462]

6. Koukourakis MI. Amifostine in clinical oncology: current use and future applications. Anticancer Drugs 2002;13:181–209. [PubMed: 11984063]
7. van der Vijgh WJF, Korst AEC. Amifostine (Ethyol): Pharmacokinetic and pharmacodynamic effects in vivo. Eur J Cancer 1996;32A:S26–S30. [PubMed: 8976819]
8. Spencer CM, Goa KL. Amifostine: A review of its pharmacodynamic and pharmacokinetic properties, and therapeutic potential as a radioprotector and cytotoxic chemoprotector. Drugs 1995;50:1001–31. [PubMed: 8612469]
9. Kemp G, Rose P, Lurain J, et al. Amifostine pretreatment for protection against cyclophosphamide-induced and cisplatin-induced toxicities: results of a randomized control trial in patients with advanced ovarian cancer. J Clin Oncol 1996;14:2101–12. [PubMed: 8683243]
10. Korst AEC, Eeltink CM, Vermorken JB, van der Vijgh WJF. Pharmacokinetics of amifostine and its metabolites in patients. Eur J Cancer 1997;33:1425–9. [PubMed: 9337685]
11. Shaw LM, Bonner HS, Schuchter L, Schiller J, Lieberman R. Pharmacokinetics of amifostine: effects of dose and method of administration. Seminars in Oncology 1999;26:34–6. [PubMed: 10348258]
12. Marina N, Chang KW, Malogolowkin M, et al. Amifostine does not protect against the ototoxicity of high-dose cisplatin combined with etoposide and bleomycin in pediatric germ-cell tumors: a Children's Oncology Group study. Cancer 2005;104:841–7. [PubMed: 15999362]
13. Fisher MJ, Lange BJ, Needle MN, et al. Amifostine for children with medulloblastoma treated with cisplatin-based chemotherapy. Pediatr Blood Cancer 2004;43:780–4. [PubMed: 15390300]
14. Fouladi M, Stempak D, Gammon J, et al. Phase I trial of a twice-daily regimen of amifostine with ifosfamide, carboplatin, and etoposide chemotherapy in children with refractory carcinoma. Cancer 2001;92:914–23. journal. [PubMed: 11550166]
15. Issels RD, Nagele A. Promotion of cystine uptake, increase of glutathione biosynthesis, and modulation of glutathione status by S-2-(3-aminopropylamino)ethyl phosphorothioic acid (WR-2721) in Chinese hamster cells. Cancer Res 1989;49:2082–6. [PubMed: 2539252]
16. Shaw LM, Bonner HS, Brown DQ. Metabolic pathways of WR-2721 (ethyol, amifostine) in the BALB/c mouse. Drug Metab Dispos 1994;22:895–902. [PubMed: 7895607]
17. Ali-Osman F, Akande O, Antoun G, Mao JX, Buolamwini J. Molecular cloning, characterization, and expression in Escherichia coli of full-length cDNAs of three human glutathione S-transferase Pi gene variants. Evidence for differential catalytic activity of the encoded proteins. JBiolChem 1997;272:10004–12.
18. Hu X, Herzog C, Zimniak P, Singh SV. Differential protection against benzo[a]pyrene-7,8-dihydrodiol-9,10-epoxide-induced DNA damage in HepG2 cells stably transfected with allelic variants of pi class human glutathione S-transferase. Cancer Res 1999;59:2358–62. [PubMed: 10344744]
19. Ishimoto TM, Ali-Osman F. Allelic variants of the human glutathione S-transferase P1 gene confer differential cytoprotection against anticancer agents in Escherichia coli. Pharmacogenetics 2002;12:543–53. [PubMed: 12360105]
20. Lien S, Larsson AK, Mannervik B. The polymorphic human glutathione transferase T1-1, the most efficient glutathione transferase in the denitrosation and inactivation of the anticancer drug 1,3-bis (2-chloroethyl)-1-nitrosourea. Biochem Pharmacol 2002;63:191–7. [PubMed: 11841793]
21. Hu X, Xia H, Srivastava SK, et al. Activity of four allelic forms of glutathione S-transferase hGSTP1-1 for diol epoxides of polycyclic aromatic hydrocarbons. Biochem Biophys Res Commun 1997;238:397–402. [PubMed: 9299520]
22. Shaw LM, Turrisi AT, Glover DJ, et al. Human pharmacokinetics of WR-2721. Int J Radiat Oncol Biol Phys 1986;12:1501–4. [PubMed: 3019968]
23. Bai F, Kirstein MN, Hanna SK, Stewart CF. New liquid chromatographic assay with electrochemical detection for the measurement of amifostine and WR1065. J ChromatogrB AnalytTechnolBiomedLife Sci 2002;772:257–65.
24. Gajjar A, Chintagumpala M, Ashley D, et al. Risk-adapted craniospinal radiotherapy followed by high-dose chemotherapy and stem-cell rescue in children with newly diagnosed medulloblastoma (St Jude Medulloblastoma-96): long-term results from a prospective, multicentre trial. Lancet Oncol 2006;7:813–20. [PubMed: 17012043]

25. Okcu MF, Selvan M, Wang LE, et al. Glutathione S-transferase polymorphisms and survival in primary malignant glioma. Clin Cancer Res 2004;10:2618–25. [PubMed: 15102663]

26. Beal, SL.; Sheiner, LB. NONMEM Project Group, University of California at San Francisco; San Francisco, CA: 1998. NONMEM Users' Guide Part I-VIII.

27. Jonsson EN, Karlsson MO. Xpose--an S-PLUS based population pharmacokinetic/pharmacodynamic model building aid for NONMEM. Comput Methods Programs Biomed 1999;58:51–64. [PubMed: 10195646]

28. Wilkins JJ. NONMEMory: a run management tool for NONMEM. Comput Methods Programs Biomed 2005;78:259–67. [PubMed: 15899310]

29. Brandt JR, Wong C, Jones DR, et al. Glomerular filtration rate in children with solid tumors: normative values and a new method for estimation. Pediatric hematology and oncology 2003;20:309–18. [PubMed: 12746163]

30. Yafune A, Ishiguro M. Bootstrap approach for constructing confidence intervals for population pharmacokinetic parameters. I: A use of bootstrap standard error. Stat Med 1999;18:581–99. [PubMed: 10209813]

31. Akcakaya H, Aroymak A, Gokce S. A quantitative colorimetric method of measuring alkaline phosphatase activity in eukaryotic cell membranes. Cell biology international 2007;31:186–90. [PubMed: 17207647]

32. Souid AK, Newton GL, Dubowy RL, Fahey RC, Bernstein ML. Determination of the cytoprotective agent WR-2721 (Amifostine, Ethyol) and its metabolites in human blood using monobromobimane fluorescent labeling and high-performance liquid chromatography. Cancer ChemotherPharmacol 1998;42:400–6.

33. Souid AK, Fahey RC, Dubowy RL, Newton GL, Bernstein ML. WR-2721 (amifostine) infusion in patients with Ewing's sarcoma receiving ifosfamide and cyclophosphamide with mesna: drug and thiol levels in plasma and blood cells, a Pediatric Oncology Group study. Cancer chemotherapy and pharmacology 1999;44:498–504. [PubMed: 10550571]

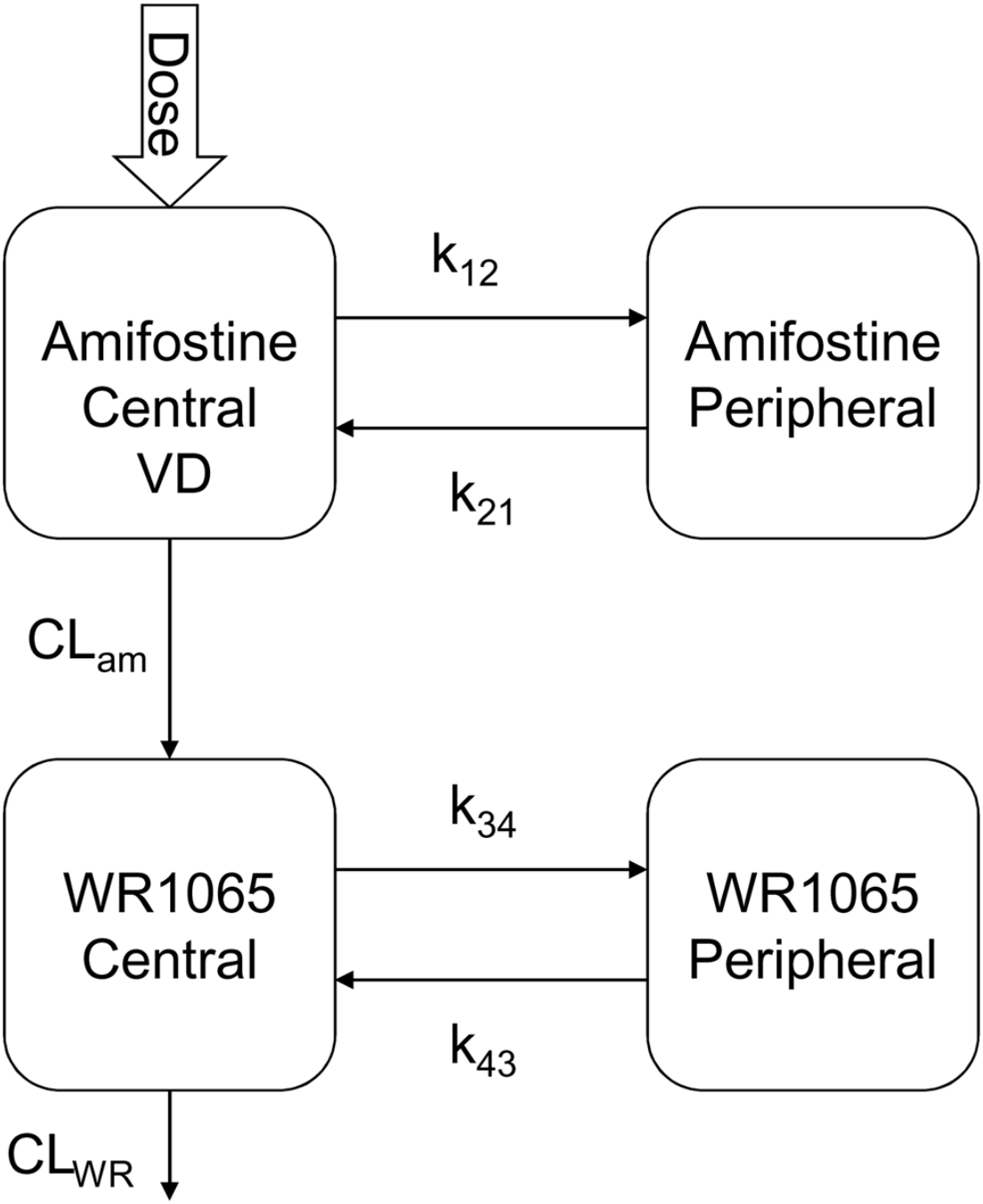


**Figure 1.**
Amifostine and WR1065 structural model

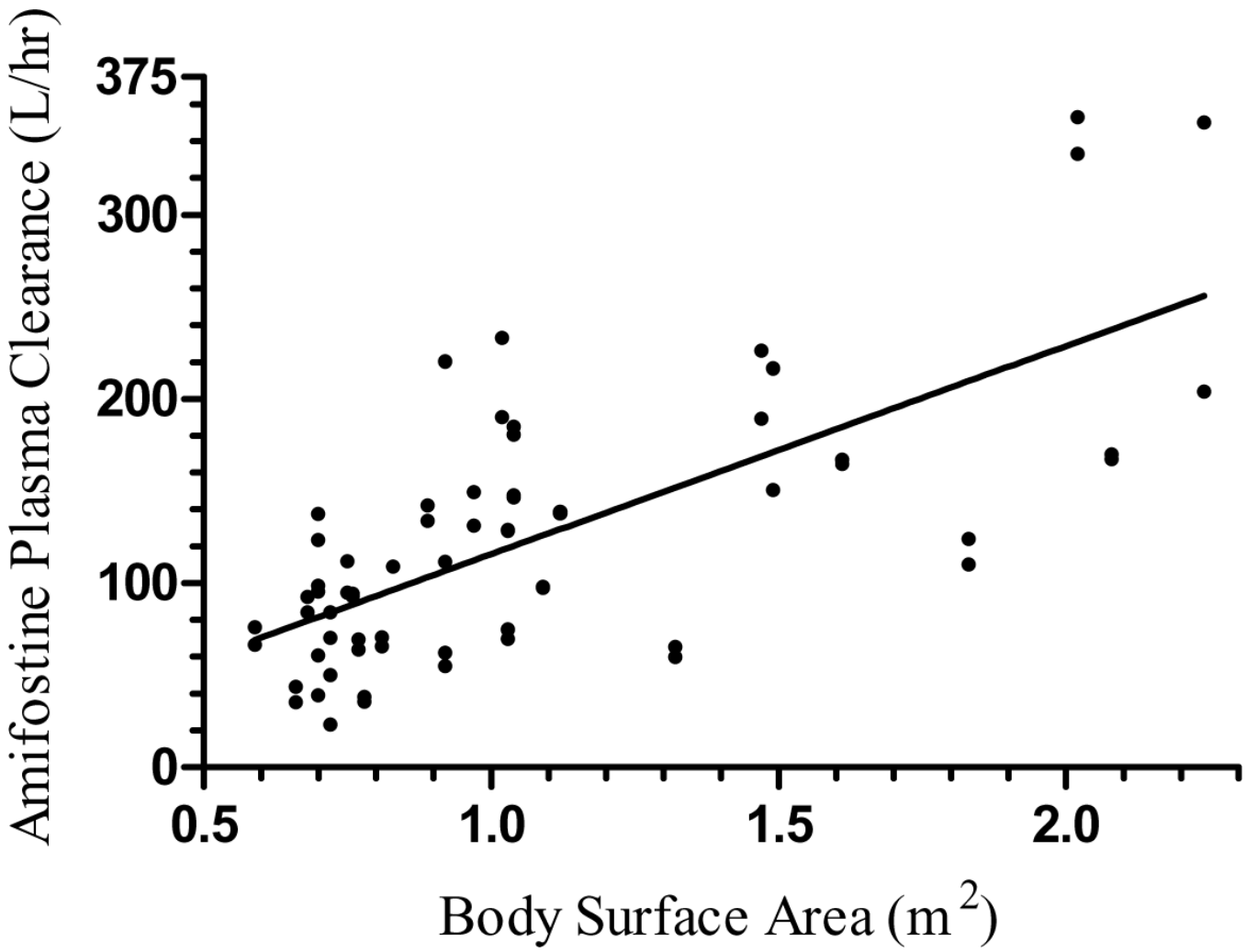


**Figure 2.**
Plot of amifostine plasma clearance vs. body surface area

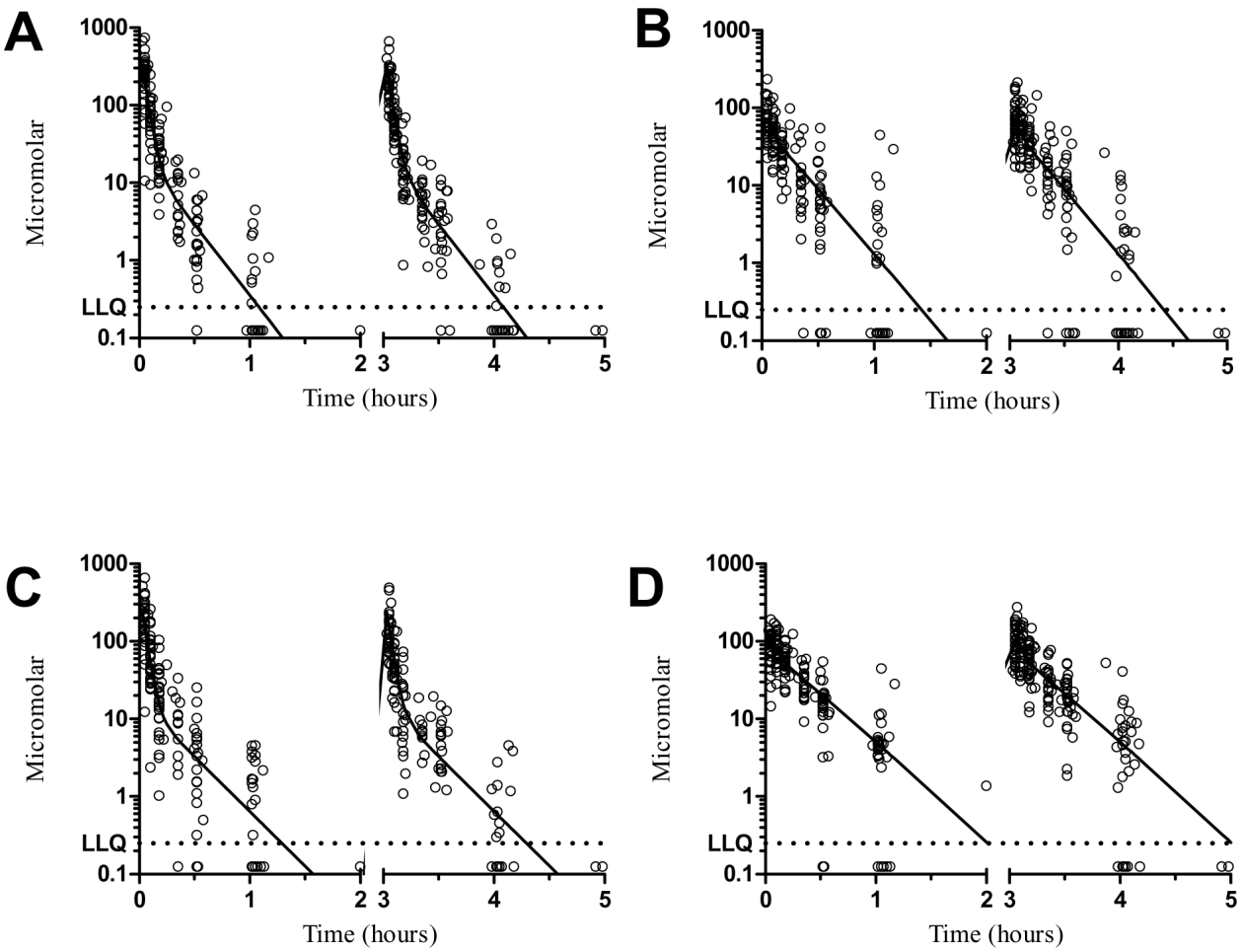


**Figure 3.**
Population estimated concentration-time curves (denoted by solid lines) and observed values (open circles) for plasma amifostine (Panel A); plasma WR1065 (Panel B); whole blood amifostine (Panel C); and whole blood WR1065 (Panel D). Observed amifostine and WR1065 concentrations below the LLQ were substituted with 0.125 (1/2*LLQ).
Abbreviation; LLQ, lower limit of quantitation

## Table 1

Baseline Patient Characteristics

| **Patient Characteristic *n* = 33** | ***n* (percent)** |
|---|---|
| Medulloblastoma Risk | |
| Category | |
| High | 20 (57) |
| Average | 13 (43) |
| Sex | |
| Male | 23 (70) |
| Female | 10 (30) |
| Race | |
| Caucasian | 31 (93) |
| Other | 2 (7) |
| GST genotype (*n* =25) | |
| M1 | |
| Present | 9 |
| null | 16 |
| T1 | |
| Present | 22 |
| null | 3 |
| P1 | |
| wt | 10 |
| variant | 15 |

| **Patient Characteristic** | **Median (range)** |
|---|---|
| Age (years) | 7.3 (3.1 – 20.1) |
| Weight (Kg) | 24.6 (13 – 96.3) |
| Height (cm) | 131 (98 – 188) |
| BSA ($m^2$) | 0.93 (0.59 – 2.24) |
| Serum creatinine (mg/dL) | 0.4 (0.3 – 0.8) |
| Albumin (g/dL) | 3.5 (3.1 – 3.9) |

Abbreviations: GST, glutathione *S*-transferase wt, wild type; BSA, body surface area

**Table 2**

Summary of Population Pharmacokinetic Parameters

| Parameter | NONMEM Estimate | Mean Bootsrap Estimate | Bootstrap SEE | Bootstrap 95% CI | NONMEM IIV (%) |
|---|---|---|---|---|---|
| $CL_{am}$ | | | | | |
| Plasma (L/hr/m$^2$)* | 107 | 106 | 8.41 | 90.3 – 123 | 0.15 (38) |
| Plasma (L/hr) | 107 | 106 | 11.5 | 86.3 – 130 | 0.31 (56) |
| Blood (L/hr/m$^2$)* | 136 | 133 | 10.7 | 113 – 155 | 0.13 (36) |
| Blood (L/hr) | 135 | 132 | 14.2 | 105 – 160 | 0.3 (55) |
| VD | | | | | |
| Plasma (L/m$^2$)* | 5.53 | 5.51 | 0.55 | 4.53 – 6.60 | 0.12 (34) |
| Plasma (L) | 5.62 | 5.51 | 0.72 | 4.36 – 7.03 | 0.32 (56) |
| Blood (L/m$^2$)* | 7.23 | 6.97 | 1.04 | 4.73 – 8.71 | 0.08 (28) |
| Blood (L) | 7.14 | 6.84 | 1.2 | 4.27 – 8.92 | 0.23 (48) |
| $CL_{WR}$ | | | | | |
| Plasma (L/hr/m$^2$)* | 30.6 | 31.3 | 4.46 | 22.4 – 40.4 | 0.34 (58) |
| Plasma (L/hr) | 30.1 | 30.9 | 4.26 | 22.4 – 39.4 | 0.34 (58) |
| Blood (L/hr/m$^2$)* | 12.5 | 13.4 | 2.87 | 9.6 – 20.5 | 0.17 (42) |
| Blood (L/hr) | 12.7 | 13.7 | 3.1 | 9.64 – 21 | 0.15 (39) |
| Population Parameters with Sex as a Covariate | | | | | |
| $CL_{am}$ | | | | | |
| Plasma (L/hr/m$^2$)* | | | | | |
| Male | 99 | 99 | 8.7 | 82.6 – 117 | 0.15 (39) |
| Δ female | 24.2 | 22.7 | 9.2 | 3.7 – 39.4 | - |
| Blood (L/hr/m$^2$)* | | | | | |
| Male | 136 | 133 | 11.2 | 112 – 158 | 0.13 (36) |
| Δ female | −0.67 | −0.08 | 12.5 | −24.7 – 26.5 | - |

| Parameter | NONMEM Estimate | Mean Bootsrap Estimate | Bootstrap SEE | Bootstrap 95% CI | NONMEM IIV (%) |
|---|---|---|---|---|---|
| VD | | | | | |
| Plasma (L/m$^2$)* | 5.41 | 5.39 | 0.56 | 4.4 – 6.52 | 0.13 (36) |
| Blood (L/m$^2$)* | 7.23 | 6.95 | 1.1 | 4.7 – 8.7 | 0.08 (28) |
| $CL_{WR}$ | | | | | |
| Plasma (L/m$^2$)* | 31.2 | 31.9 | 4.5 | 23 – 40.8 | 0.33 (57) |
| Blood (L/m$^2$)* | 12.5 | 13.4 | 2.9 | 9.7 – 20.9 | 0.17 (41) |

Abbreviations: SEE, standard error of the estimate; 95% CI, percentile bootstrap 95% confidence interval; IIV, interindividual variability; Δ female, population estimated difference in clearance in female patients

* indicates estimate from body surface area normalized model

## Table 3

Proportional Residual Error in Plasma and Whole Blood Pharmacokinetic Models

| BSA-Normalized Models | Amifostine Residual Error (%) | WR1065 Residual Error (%) |
|---|---|---|
| Plasma | | |
| Without IOV | 0.19 (43) | 0.20 (44) |
| With IOV | 0.13 (37) | 0.19 (44) |
| With sex and IOV | 0.19 (44) | 0.13 (35) |
| Whole blood | | |
| Without IOV | 0.33 (57) | 0.12 (34) |
| With IOV | 0.19 (44) | 0.13 (35) |
| With sex and IOV | 0.19 (44) | 0.13 (35) |

Abbreviations: BSA, body surface area; IOV, interoccasion variability.